Interplanetary magnetic field control of the location of substorm onset and auroral features in the conjugate hemispheres

N. Østgaard, S. B. Mende, H. U. Frey, and T. J. Immel

Space Sciences Laboratory, University of California, Berkeley, California, USA

L. A. Frank and J. B. Sigwarth

Department of Physics and Astronomy, University of Iowa, Iowa City, Iowa, USA

T. J. Stubbs

Laboratory for Extraterrestrial Physics, NASA Goddard Space Flight Center, Greenbelt, Maryland, USA

[1] During 2001 and 2002, when the Imager for Magnetopause-to-Aurora Global Exploration (IMAGE) satellite had its apogee in the Northern Hemisphere and the Polar spacecraft, owing to the apsidal precession of its orbit, reached higher altitudes in the Southern Hemisphere, the two spacecraft offered a unique opportunity to study the aurora in the conjugate hemispheres simultaneously. Owing to the large fields of view of the Polar Visible Imaging System (VIS) Earth camera and the IMAGE-FUV instruments, substorms and auroral features were imaged on a global scale in both hemispheres. We have identified five substorm onsets and several auroral features that can be unambiguously identified and compared in the two hemispheres. When mapped onto apex coordinates in the two hemispheres, we find that substorm onset locations and auroral features are usually not symmetric. The longitudinal displacement in one hemisphere compared with the other can be as much as 1.5 hours of local time ($\sim$1500 km). For southward interplanetary magnetic field (IMF) the hemispherical asymmetry (ΔMLT) is strongly correlated with the IMF clock angle (θ_C) and a linear fit, ΔMLT $= -0.017\theta_C + 3.44$, gives a correlation coefficient of 0.83 with a mean deviation of 0.4ΔMLT. These findings are interpreted as the magnetic tensions force acting on open magnetic field lines before reconnecting in the magnetotail. This can also be thought of as the IMF penetrating the magnetosphere.   *INDEX TERMS:* 2740 Magnetospheric Physics: Magnetospheric configuration and dynamics; 2784 Magnetospheric Physics: Solar wind/magnetosphere interactions; 2704 Magnetospheric Physics: Auroral phenomena (2407); 2788 Magnetospheric Physics: Storms and substorms; 2730 Magnetospheric Physics: Magnetosphere—inner; *KEYWORDS:* substorm onset, conjugate, aurora, IMF, asymmetry, nightside reconnection

Citation: Østgaard, N., S. B. Mende, H. U. Frey, T. J. Immel, L. A. Frank, J. B. Sigwarth, and T. J. Stubbs (2004), Interplanetary magnetic field control of the location of substorm onset and auroral features in the conjugate hemispheres, *J. Geophys. Res.*, *109*, A07204, doi:10.1029/2003JA010370.

1. Introduction

[2] The expectation of observing similar auroral features simultaneously in the conjugate hemispheres arises from the fact that charged particles are "tied" to magnetic field lines owing to their gyromotion on the timescale of their mirroring period (a few seconds) from one hemisphere to the other. If the magnetic field lines connecting the two hemispheres were symmetric, as they would be in a simple dipole field, any disturbance/instability in the magnetosphere that causes particles to precipitate in the ionosphere

would result in auroral features that could be observed at exactly the same geomagnetic locations in the Southern and Northern Hemispheres. On the other hand, if the magnetotail were twisted (i.e., rotated around the Sun-Earth line), the pair of foot points of the nightside field lines will have different geomagnetic coordinates (e.g., apex, corrected geomagnetic). Precipitation at the foot points of such a field line in the two hemispheres will appear as nonconjugate phenomenon (in geomagnetic coordinates), although it occurs on the same field line. In the literature, such observations are sometimes defined as nonconjugate phenomena. For example, in the study by *Stenbaek-Nielsen and Otto* [1997] where the results from *Stenbaek-Nielsen et al.* [1972, 1973] are revisited, they conclude that while the

diffuse aurora seems to be conjugate, the discrete aurora seems to be nonconjugate. In order to account for the asymmetry of similar auroral features in the conjugate hemispheres, they argue that the magnetotail must be twisted when the interplanetary magnetic field (IMF) has a significant B_y component penetrating the magnetosphere. On the other hand, if one wants to compare in situ measurements in space with ionospheric observations, conjugacy would usually be defined as being on the same field line. Consequently, there seems to be some ambiguity in the literature about what conjugacy is. We will therefore define conjugacy and a conjugate phenomenon as a phenomenon that occurs on the same magnetic field line, connecting the two hemispheres, even though the foot points of the field line may have different geomagnetic coordinates. A nonconjugate phenomenon would be auroral features that are observed in one hemisphere but not in the other (i.e., not connected). Following this, we will rather use the term asymmetric geomagnetic locations for phenomena, like substorm onset, that occur on the same magnetic field line but displaced in the two hemispheres.

[3] Owing to the very few observation sites in the Southern Hemisphere and the requirements of darkness and clear sky in both hemispheres, simultaneous conjugate ground-based optical observation are rare [*Sato et al.*, 1998]. To overcome poor observation conditions at certain ground stations, a series of conjugate aircraft flights equipped with all-sky imagers was undertaken [*Stenbaek-Nielsen et al.*, 1972, 1973]. Another approach has been to utilize imaging from space in one hemisphere combined with ground-based optical observations in the other [e.g., *Burns et al.*, 1990; *Vorobjev et al.*, 2001]. Recently, *Frank and Sigwarth* [2003] showed observations of an auroral onset in both hemispheres by the Visible Imaging System (VIS) Earth camera on board the Polar spacecraft. The imagers on board DE-1 and Viking also observed the nightside aurora simultaneously in the two hemispheres [e.g., *Pulkkinen et al.*, 1995]. Although early studies with all-sky cameras reported similarity in the spatial and temporal development in both hemisphere [*Belon et al.*, 1969; *Fujii et al.*, 1987], we have sufficient evidence by now that this is not always the case. Some studies have supported these early findings [*Pulkkinen et al.*, 1995; *Frey et al.*, 1999], but other studies have clearly demonstrated that auroral nightside features may be largely displaced in the two hemispheres [*Sato et al.*, 1986; *Burns et al.*, 1990; *Stenbaek-Nielsen and Otto*, 1997; *Frank and Sigwarth*, 2003]. Displacements have been found both in latitude and longitude [*Stenbaek-Nielsen and Otto*, 1997], although the longitudinal displacement seems to be the most pronounced and range from a few hundreds of kilometers [*Sato et al.*, 1986, 1998; *Frank and Sigwarth*, 2003] up to 1–2 magnetic local time (MLT) sectors [*Burns et al.*, 1990]. Latitudinal and longitudinal displacements as well as dif-

ference in auroral intensities have been attributed to magnetospheric currents or more direct IMF influence on the magnetospheric field configuration [*Burns et al.*, 1990; *Stenbaek-Nielsen and Otto*, 1997; *Vorobjev et al.*, 2001]. Nonconjugate auroras, meaning occurrence of auroral features in one hemisphere only, have been attributed to asymmetric field-aligned currents resulting from differences in ionospheric conductivity [*Stenbaek-Nielsen et al.*, 1972; *Sato et al.*, 1998]. While it has been well documented that IMF controls the dayside aurora and cusp aurora location [e.g., *Sandholt et al.*, 1998; *Sandholt and Farrugia*, 1999], only a few studies indicate that the IMF also controls the location of the nightside aurora [*Elphinstone et al.*, 1990; *Liou et al.*, 2001]. More observations and studies are needed to resolve to what extent and how the IMF controls nightside auroral features and substorm onsets in the two hemispheres [*Vorobjev et al.*, 2001].

[4] During 2001 and 2002 the Polar and Imager for Magnetopause-to-Aurora Global Exploration (IMAGE) spacecraft offered a unique opportunity to study the aurora simultaneously in the conjugate hemispheres. Owing to the apsidal precession of the Polar spacecraft orbit and the large field of view of the Polar VIS Earth camera and the IMAGE-FUV instruments, substorms and auroral features were imaged on a global scale from the Southern (VIS Earth camera) and the Northern (IMAGE-FUV) Hemispheres simultaneously. Mapped onto magnetic apex coordinates [*Richmond*, 1995], we show that substorm onset location and auroral features are usually not symmetric. Combined with IMF data from Wind and ACE, we present strong evidence of IMF control of the hemispherical asymmetry.

2. Observations

[5] We have identified five substorm onsets and six auroral features that can be unambiguously determined and compared in the conjugate hemispheres. In this section we will present two of the substorms and one of the features in detail and then give an overview of the times, types, and IMF conditions for all the observations.

2.1. The 13 September 2001 Event

[6] Figure 1 shows a substorm that occurred on 13 September 2001 at 0943 UT. The quick-look AE index from Kyoto World Data Center (Figure 1d) displays a typical substorm signature reaching a maximum of 470 nT. In Figures 1a–1c the IMAGE FUV Wideband Imaging Camera (WIC) images from the Northern Hemisphere are shown to the left and VIS Earth camera images from the Southern Hemisphere are shown to the right. The emission height is taken to be 130 km and apex magnetic coordinates are used for the mapping. The apex coordinate system is based on the Definite/International Geomagnetic Reference Field (DGRF/IGRF) and does not take into account any asymme-

Figure 1. The 13 September 2001 event. (a)–(c) Imager for Magnetopause-to-Aurora Global Exploration (IMAGE) Wideband Imaging Camera (WIC) images from the Northern Hemisphere and Visible Imaging System (VIS) Earth images from the Southern Hemisphere mapped onto apex magnetic coordinates. (d) The quick-look AE index from Kyoto, Japan. (e) The peak (thick) and the 50% intensity contour (thin) local time location for the substorm onset in the Southern (dashed) Hemisphere and the Northern (solid) Hemisphere. (f) The interplanetary magnetic field (IMF) in GSM coordinates measured by Wind (solid) and ACE (dashed) time-shifted to X= −10 R_E.
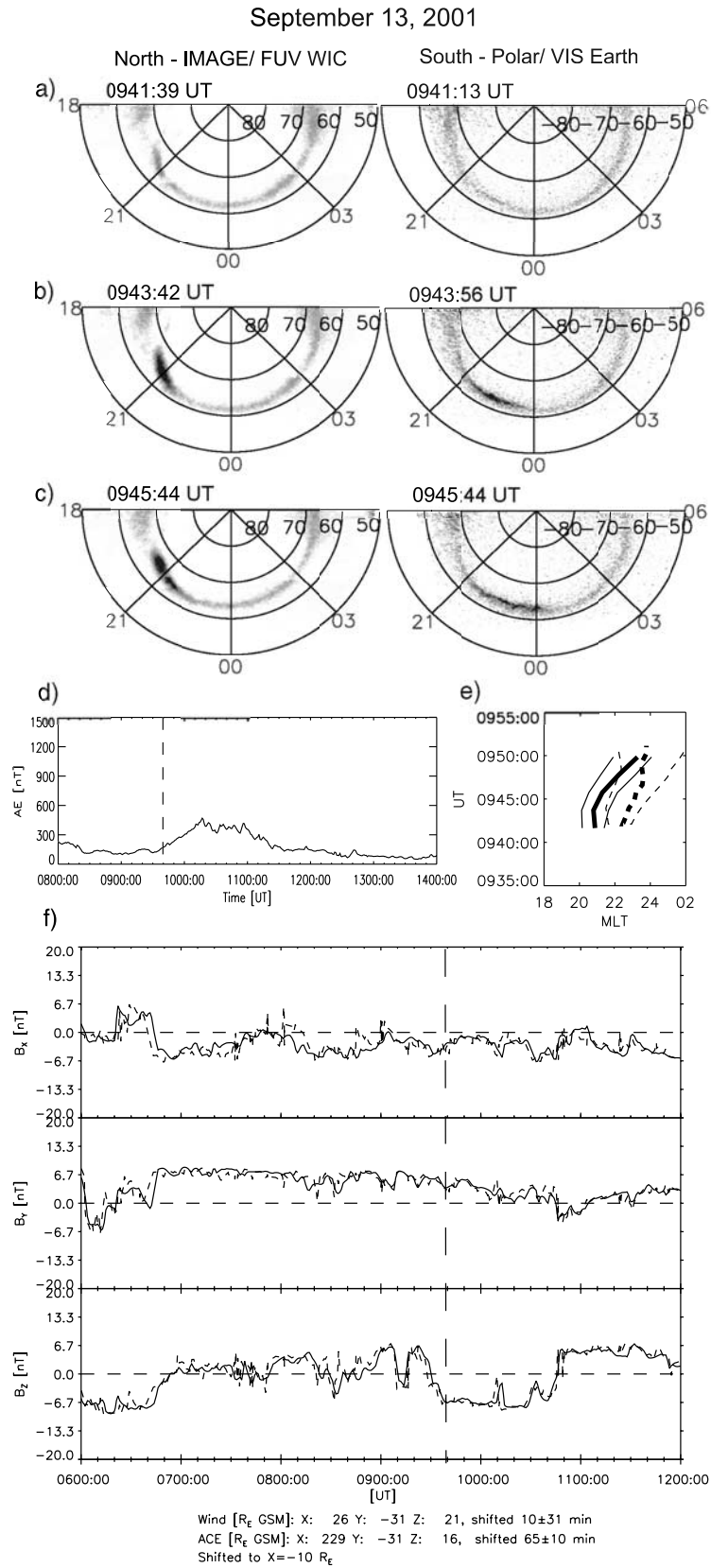
Figure 1

tries imposed by external fields. Although the VIS Earth camera images (130.4 nm) should, strictly speaking, be compared with IMAGE SI13 (135.6 nm) as they both are O I emissions, we have decided to present IMAGE WIC images (140–180 nm), owing to their higher count rates, after checking that the onset location in the WIC images does not differ from what is observed in the SI13 images. Exposure times are 10 s and 32.5 s for IMAGE WIC and VIS Earth camera, respectively, and the center time of integration is used to label the images. From the images in Figure 1b we locate the substorm auroral breakup in the Northern Hemisphere at ∼2100 MLT and at ∼2230 MLT in the Southern Hemisphere. Figure 1e illustrates the time history of the peak intensities (thick line) and the 50% intensity contour (thin line). For the first 5–10 min after the substorm breakup, a 1.6 MLT dawnward displacement of the onset in the Southern Hemisphere (dashed lines) relative to the Northern Hemisphere (solid lines) is recorded. The time-shifted IMF data from Wind and ACE (Figure 1f) show almost identical field variations with a negative B_z and a positive B_y at the time corresponding to the substorm onset and expansion phase. In order to examine any IMF influence on the inner nightside magnetosphere, the IMF data are radially time-shifted (point by point) to X = −10 R$_E$, although a larger time shift to, e.g., −20 R$_E$ would have given approximately the same results. Using a 10 min average (of the time-shifted data) centered around the onset time, the IMF B_z and B_y from Wind (ACE) are found to be −6.4 (−6.4) nT and 4.2 (4.4) nT, respectively. We notice that a positive B_y is accompanied by a dawnward displacement of the southern substorm onset.

2.2. The 15 November 2001 Event

[7] In Figure 2 the substorm on 15 November 2001 at 1720 UT is presented in a similar format as the first event. The quick-look AE index indicates a rather intense substorm reaching a maximum of 1000 nT. The WIC image in Figure 2b shows that the breakup in the Northern Hemisphere occurs at 2330 MLT, while the auroral breakup in the Southern Hemisphere is slightly duskward of that. Identifying peak intensities from the images in the conjugate hemispheres, we find a 0.5 MLT duskward displacement of the southern onset location relative to the northern onset. As the Wind satellite was located inside the magnetopause during this event, we only have ACE data to determine the IMF orientation. The 10-min averaged B_z and B_y components were both clearly negative (−11.1 nT and −8.3 nT, respectively). A negative B_y is accompanied by a duskward displacement of the southern substorm onset.

2.3. The 2 July 2001 Event

[8] Listed in Table 1 are data from three more substorms analyzed in this study. Although a total of five events does provide a minimally statistically significant sample, considering how hard it is to find the two spacecraft located in the right hemispheres at the right times, more events are needed to obtain statistical information about any IMF influence on the hemispherical asymmetry. We have therefore looked for auroral features that can be unambiguously determined in both the Northern and the Southern Hemispheres. Such features can be sudden brightenings with characteristic shapes or a westward/eastward expanding bulge with sharp

intensity gradients at the leading edge. Figure 3 displays three time frames from 2 July 2001, 0421–0431 UT, where features in the conjugate hemispheres can be well matched up with each other. In Figure 3a an S-shaped aurora is seen in the 2200–2400 MLT sector in the Northern Hemisphere, while a similar S-shaped feature reaches all the way to 2100 MLT in the Southern Hemisphere. In the next two frames a westward expanding bulge in the Southern Hemisphere is observed about one local time sector duskward of where the bulge is seen in the Northern Hemisphere. The three time frames display auroral features in the Southern Hemisphere about one local time sector duskward of the similar feature in the Northern Hemisphere. Steady IMF conditions show a weak negative B_z component (Wind: −0.7 nT, ACE: −2.2 nT) and a large negative B_y (−8.2 nT or −8.5 nT). A negative B_y is accompanied by a duskward displacement of the S-shaped feature and the bulge in the Southern Hemisphere.

2.4. Overview

[9] Table 1 lists all the observations analyzed in this study, which encompasses five substorm onsets and six auroral features. We have also included the event reported by *Frank and Sigwarth* [2003] where a 40 min dawnward displacement was found for the southern auroral breakup. One may notice that the IMF values on 1 November 2001 (event 4 in Table 1) are slightly different from what *Frank and Sigwarth* [2003] reported. Similar steady IMF conditions were recorded by both Wind and ACE for hours, and we feel confident about the values we have used. For all the events we have assumed a simple planar propagation when the IMF data have been shifted in time. In most cases the solar wind data are either slowly varying or the two spacecraft report similar IMF variations. The uncertainties of our time shifts are in the range of 0–10 min [*Collier et al.*, 1998], consistent with the 10 min averages of the IMF data we use. Events where the IMF cannot be determined have not been included. The trend (except events 1, 7, and 12, which will be discussed below) is that dawnward (duskward) displacements in the Southern Hemisphere are associated with a positive (negative) B_y.

[10] To display the correlation between IMF and the relative displacements in the conjugate hemispheres, we have plotted the displacements versus IMF clock angle and IMF B_y. Figures 4a and 4b display the displacement (at 130 km altitude) in ΔMLT and Δkm (in azimuth), respectively, as a function of IMF clock angle (Figure 4d). The latter (Δkm) takes into account the average latitude where the features are seen without changing the picture very much. Figure 4c shows the displacement as a function of B_y. Squares are used for the onsets and diamonds are used for the features. Including the result from *Frank and Sigwarth* [2003], we have a total of 12 events. ACE data (grey) were available for all the events, while data from Wind are used only when the satellite is outside the magnetopause and not too far from the Sun-Earth line (|Y| < 40 R$_E$). In order to use all the IMF measurements and to weight all events equally, we have given the events where only ACE measurements were available double weight. This gives us a total of 24 data points and the linear fits to the data versus clock angle give a 0.72 correlation coefficient for both ΔMLT and Δkm, with
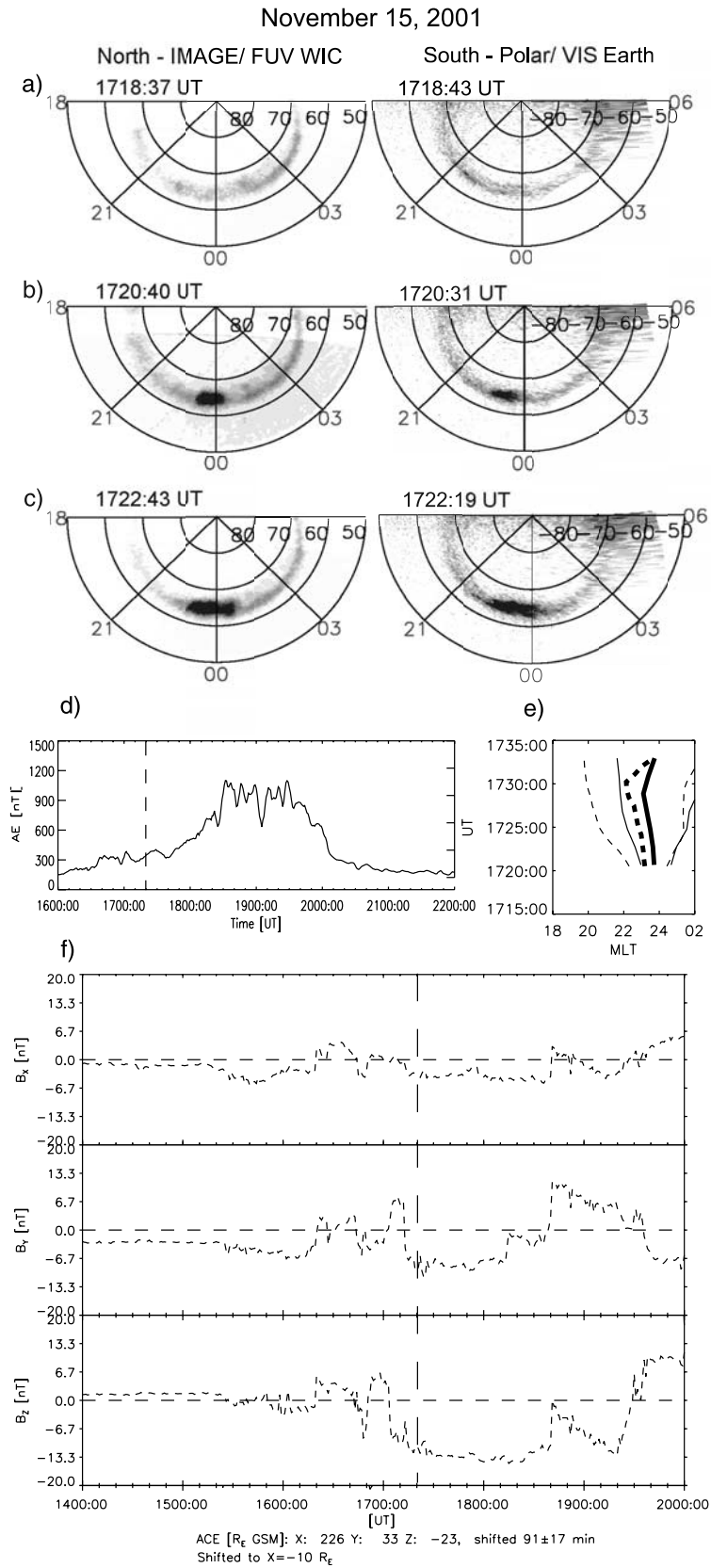
Figure 2. Same as Figure 1 but for 15 November 2001.

Table 1. Times, Type of Feature, Interplanetary Magnetic Field (IMF), and Relative Longitudinal Displacement

	Date	Time	Type	IMF B_z[a]	IMF B_y[a]	ΔMLT[b]	MLT[c]
1	010705	0603	Onset	(−3.9)	(−4.4)	0.6	21.0
2	010913	0943	Onset	−6.4 (−6.4)	4.2 (4.4)	1.6	21.5
3	011022	0718	Onset	0.1 (−2.2)	−4.3 (−5.0)	−1.4	21.0
4	011101[d]	1153	Onset	−9.0 (−9.7)	6.1 (6.2)	0.7	23.0
5	011115	1720	Onset	(−11.0)	(−8.3)	−0.5	23.5
6	021023	1056	Onset	−2.7 (0.9)	−1.7 (−5.1)	−0.7	22.5
7	010512	2126	Huge local intensification	(−3.1)	(−0.1)	0.8	19.5
8	010702	0430	Westward bulge	−0.7 (−2.2)	−8.2 (−8.5)	−1.1	23.0
9	011115	1805	Westward bulge	(−13.8)	(−7.2)	−0.5	21.0
10	011115	1824	Westward bulge	(−13.5)	(−2.2)	−0.2	20.0
11	021023	1146	Intensification	1.3 (0.3)	−3.8 (−4.8)	−1.1	21.0
12	021207	1413	Intensification	2.7 (1.3)	−9.8 (−6.9)	0.1	22.2

[a]Wind (ACE), Wind data are not used when the satellite is inside the magnetopause or far off the Sun-Earth line.
[b]Positive when southern feature is dawnward of the northern feature.
[c]Average magnetic local time (MLT) position.
[d]The substorm reported by *Frank and Sigwarth* [2003].

a mean deviation of 0.5ΔMLT and 390Δkm, respectively. The linear fit to the data versus B_y gives a slightly lower correlation of 0.67 with a mean deviation of 0.6ΔMLT. The ΔMLT (or Δkm) correlates poorly (<0.4) with the dipole tilt angle (not shown).

3. Discussion

[11] An interpretation that is consistent with the afore-mentioned relationships would be the magnetic tension force due to a duskward or dawnward directed IMF acting on open field lines before they reconnect in the magnetotail. This is visualized in Figure 5a, where we have sketched a snapshot of two pairs of open field lines (thin solid and dashed/dotted) and one closed field line (thick solid). Given a southward IMF with $B_y > 0$ (like on 13 September), the tension force (thick grey arrows) is oppositely directed in the conjugate hemispheres, i.e., toward dusk in the Southern Hemisphere and toward dawn in the Northern Hemisphere. This means that open field lines with symmetric foot points, like the thin solid lines, will be pulled away from each other as they convect from dayside to nightside and will not be able to "find" each other in the tail. On the other hand, open field lines with certain asymmetric foot points like the dashed and dotted lines will be pushed toward each other by the tension force as they move from the dayside to the nightside and are able to reconnect in the tail. It should be noticed that the tension force acting on open field lines will be strongest on the dayside [*Sato et al.*, 1998], a feature also known from ionospheric polar cap plasma convection patterns for different signs of B_y [e.g., *Kelley*, 1989, pg. 292]. The thick line depicts a newly reconnected (closed) field line which has highly asymmetric foot points. The sketch illustrates the case where the southern onset is dawnward of the northern onset like on 13 September 2001. Such an interpretation, where the magnetic tension force plays the dominant role, implies that the hemispherical displacements should be correlated not only with IMF B_y but with the ratio of B_y/B_z or the IMF clock angle, in nice agreement with Figure 4, where the highest correlation is found for ΔMLT versus clock angle. A similar interpretation is discussed by *Vorobjev et al.* [2001], who attributed longitudinal displacements to the magnetic tension force resulting from IMF B_y component pulling newly opened field lines in opposite directions in the two hemispheres.

One may also think of this as the penetration of IMF B_y [e.g., *Cowley et al.*, 1991; *Stenbaek-Nielsen and Otto*, 1997], as simply sketched in Figure 5b. The solid line is the symmetric field line, while the dashed line is the resulting field line when IMF B_y is superimposed. This picture also can illustrate why the foot point in the Northern Hemisphere will be duskward of the southern foot point (when $B_y > 0$). The penetration of IMF B_y will twist the field line configuration in the magnetotail, which has been confirmed by in situ measurements [*Sibeck*, 1985; *Wing et al.*, 1995] and can explain the difference in discrete aurora locations in the two hemispheres. *Stenbaek-Nielsen and Otto* [1997] suggested that the IMF B_y penetration will only affect the outer magnetosphere, setting up an interhemispherical current from north (south) to south (north) for $B_y < 0$ ($B_y > 0$) that would add to (subtract from) the upward evening region 1 current in the Northern (Southern) Hemisphere. They argued that this could explain why the auroral intensities as well as the latitudinal location can be different in the two hemispheres. Although the concept of the IMF penetration is also based on the stresses exerted on the magnetosphere consequent on the interconnection of terrestrial and interplanetary fields [*Cowley et al.*, 1991], the B_y component has been considered to be the controlling parameter [*Stenbaek-Nielsen and Otto*, 1997]. Our results indicate that IMF penetration is not restricted to the outer magnetosphere. Our events are observed at magnetic latitudes ranging from 60° to 69°, indicating source regions in the inner magnetosphere, in agreement with IMF penetration observed at geosynchronous orbits [*Wing et al.*, 1995]. Our observations also give a slightly higher linear correlation coefficient and smaller mean deviation with the IMF clock angle (0.72 and 0.5ΔMLT) than with B_y alone (0.67 and 0.6ΔMLT), which may indicate that both B_y and B_z are important for the IMF control of the relative displacement of onsets and features in the conjugate hemisphere. The relative displacement (ΔMLT) versus IMF clock angle can be expressed as

$$\Delta MLT = -0.013\theta_C + 2.82, \tag{1}$$

where θ_C is clock angle in degrees, defined in Figure 4d.

[12] The poor correlation found for ΔMLT versus dipole tilt angle (not shown) is consistent with the expected tilt-related effects on the tail configuration. As discussed by
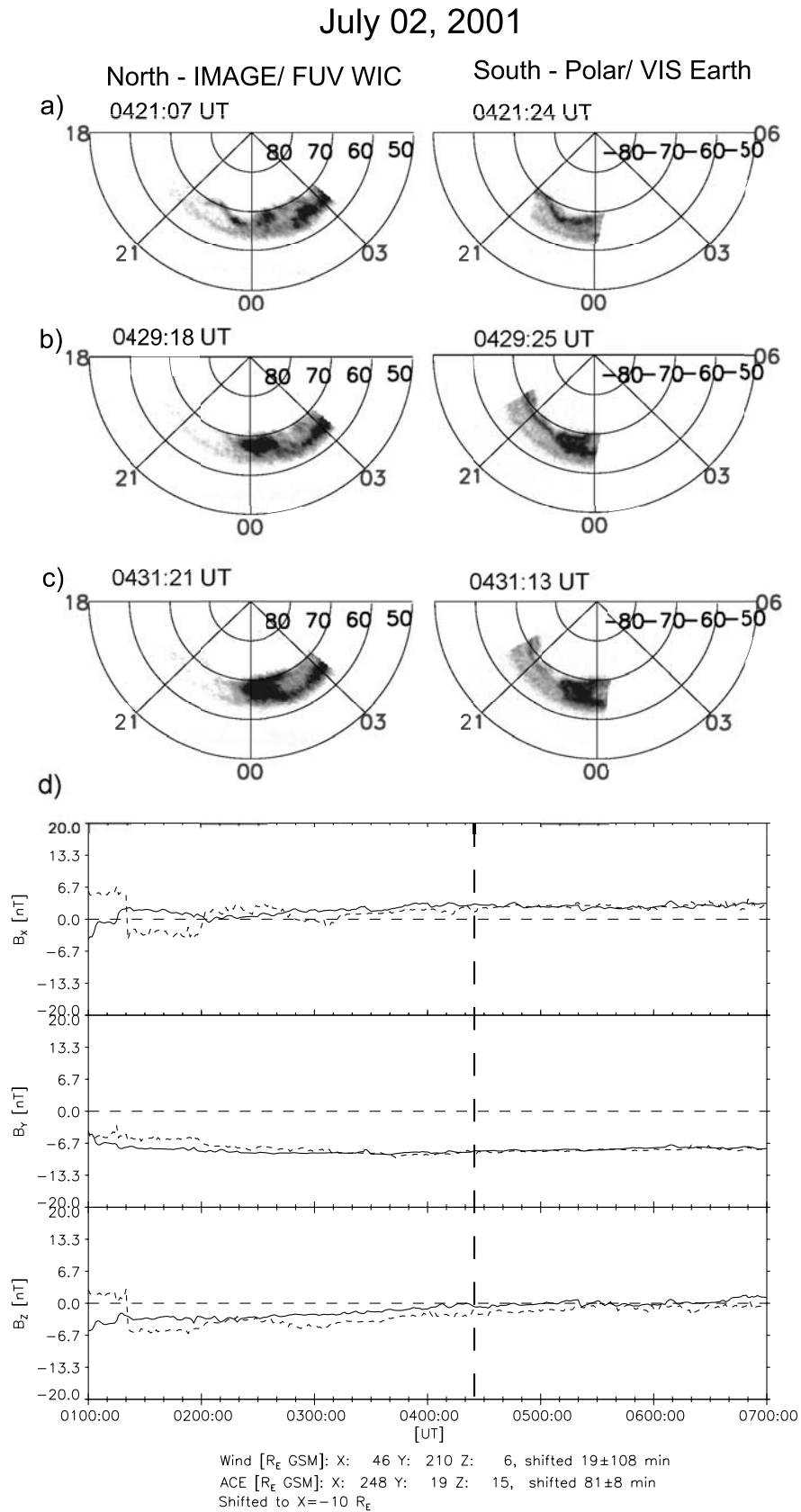
Figure 3. The 2 July 2001 event. (a)–(c) Images from the conjugate hemispheres. (d) IMF. See color version of this figure at back of this issue.
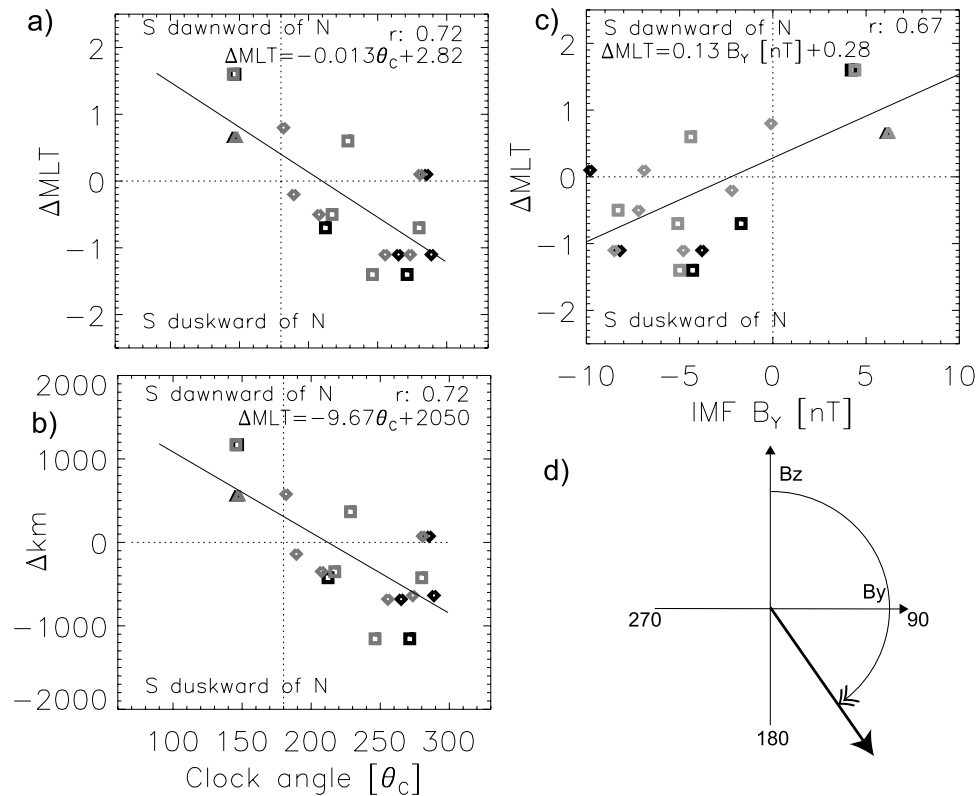
Figure 4. The relative displacement of the onset locations (squares) and auroral features (diamonds) in the two hemispheres versus IMF measured by Wind (black) and ACE (grey). The triangle is the displacement (40 min at 59° magnetic latitude) during the 1 November 2001 substorm reported by *Frank and Sigwarth* [2003]. (a) ΔMLT versus θ_C (clock angle). (b) Δkm versus θ_C. (c) ΔMLT versus B_y. (d) Clock angle definition.

Tsyganenko [1998], the dipole tilt angle will lead to warping (and not twisting) of the tail and will not lead to a systematic displacement but only affect aurora with source regions on the flanks of the magnetosphere.

[13] In view of the interpretation given above, we want to comment on the four data points in Figure 4, where a negative B_y (or $\theta_C > 180°$) is associated with a positive displacement. These are the four data points in the upper right (left) quadrant in Figures 4a and 4b (Figure 4c). The event on 12 May 2001 (event 7, ΔMLT = 0.8, $B_y = -0.1$ nT, $B_z = -3.2$ nT $\theta_C = \sim180°$) was a huge local intensification in the dusk sector (1900 MLT). Following the concept of stresses on field lines due to the tension force or what is expected from the "dipole plus uniform IMF" [*Cowley*, 1981], one may argue that the B_x component should have some influence on latitudinal displacement in the noon-meridian plane [*Vorobjev et al.*, 2001] and on longitudinal displacement for auroras with source regions on the flanks. During this event, the B_x component is large (8.3 nT) compared with both B_z (−3.1 nT) and B_y (−0.1 nT) and could be responsible for an eastward (or dawnward) displacement of the southern features in the dusk sector. Consequently, the displacement for this event may be more affected by the B_x than by B_y. An alternate explanation is that the warping of the tail caused by the large positive dipole tilt angle (22°) can result in a dawnward displacement of the duskside aurora in the Southern Hemisphere [*Tsyganenko*, 1998].

[14] The event on 7 December 2002 (event 12, ΔMLT = 0.1, $B_y = -9.8$ (−6.9) nT, $\theta_C = \sim280$ (285°)) is the only event that occurs when both Wind and ACE measure a relatively long period (>1 hour) of significant positive B_z (2.7 nT and 1.3 nT). In this case we may have lobe reconnection, and the tension force will not affect the inner magnetotail. This may explain why these data points deviate clearly from the linear fit. If these two data points were excluded from the data set, we would have 11 events and 22 data points (with the double weighting described above) and obtain linear fits with linear correlation coefficients and mean deviations of $0.83-0.4\Delta$MLT (ΔMLT versus θ_C), $0.82-340\Delta$km (Δkm versus θ_C), and $0.75-0.6\Delta$MLT (ΔMLT versus B_y). As shown in Figure 6, the linear fit would then become

$$\Delta\text{MLT} = -0.017\theta_C + 3.44. \qquad (2)$$

For the event on 5 July 2001 (event 1, ΔMLT = 0.6, $B_y = -3.9$ nT, $\theta_C = \sim230°$), we have no explanation why this data point deviates from the linear fit.

4. Conclusions

[15] In the open magnetospheric model, first suggested by *Dungey* [1961], the IMF is an important controlling factor of solar wind magnetosphere coupling. From plasma convection patterns in the polar cap [*Kelley*, 1989], dayside

merging, and cusp aurora location [*Sandholt et al.*, 1998], the importance of the IMF orientation for this coupling has been well documented. Previous studies have indicated that the IMF can penetrate the outer [*Sibeck*, 1985] as well as the inner [*Wing et al.*, 1995] magnetosphere. A few studies have also reported that the IMF affects the location of the aurora [*Elphinstone et al.*, 1990; *Liou et al.*, 2001; *Vorobjev et al.*, 2001]. Owing to the very few observations of conjugate aurora from space or from space combined with ground measurement, it has not been possible to determine more quantitatively the IMF control of the relative displacement of the aurora in the conjugate hemispheres.

[16] On the basis of imaging data from the Polar VIS Earth camera and the IMAGE-FUV instruments, we have presented substorm onsets and auroral features that can be identified unambiguously from global scale images in both hemispheres. We have documented that for southward IMF there exists a systematic hemispherical asymmetry, which is strongly correlated with the IMF clock angle. The relative displacement (ΔMLT) can be expressed as a linear function of IMF clock angle. In a future study we will examine how well this asymmetry is incorporated in the few magnetic field models that has taken into account the IMF affect on
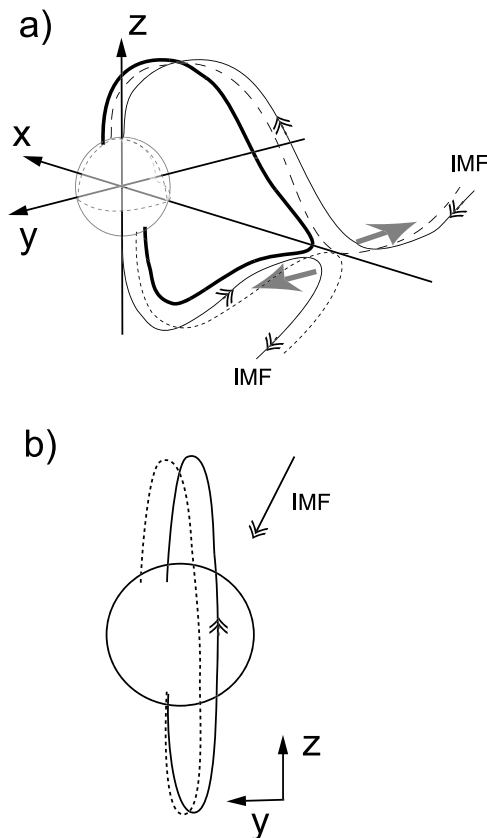

Figure 6. Same as Figure 4a but with the two data points where IMF B_z is clearly positive removed.

the inner magnetosphere [*Toffoletto and Hill*, 1989, 1993; *Tsyganenko*, 2002a, 2002b].

References

Belon, A. E., J. E. Maggs, T. N. Davis, K. B. Mather, N. W. Glass, and G. F. Hughes (1969), Conjugacy of visual auroras during magnetically quiet periods, *J. Geophys. Res.*, *74*, 1–28.
Burns, G. B., D. J. McEwen, R. A. Eather, F. T. Berkey, and J. S. Murphree (1990), Optical auroral conjugacy: Viking UV imager-South Pole station ground data, *J. Geophys. Res.*, *95*, 5781–5790.
Collier, M. R., J. A. Slavin, R. P. Lepping, A. Szabo, and K. Ogilvie (1998), Timing accuracy for the simple planar propagation magnetic field structures in the solar wind, *Geophys. Res. Lett.*, *25*(14), 2509–2512.
Cowley, S. W. H. (1981), Magnetospheric asymmetries associated with the Y-component of the IMF, *Planet. Space Sci.*, *29*, 79.
Cowley, S. W. H., J. P. Morelli, and M. Lockwood (1991), Dependence of convective flows and particle precipitation in the high-latitude dayside ionosphere and the X and Y components of the interplanetary magnetic field, *J. Geophys. Res.*, *96*, 5557–5564.
Dungey, J. W. (1961), Interplanetary magnetic field and the auroral zones, *Phys. Rev. Lett.*, *6*, 47–48.
Elphinstone, R. D., K. Jankowska, J. Murphree, and L. Cogger (1990), The configuration of the auroral distribution for interplanetary magnetic field-B_z northward: 1. IMFB_x and B_y dependencies as observed by the VIKING satellite, *J. Geophys. Res.*, *95*, 5791.
Frank, L. A., and J. B. Sigwarth (2003), Simultaneous images of the northern and southern auroras from the Polar spacecraft: An auroral substorm, *J. Geophys. Res.*, *108*(A4), 8015, doi:10.1029/2002JA009356.
Frey, H. U., S. B. Mende, H. B. Vo, M. Brittnacher, and G. K. Parks (1999), Conjugate observation of optical aurora with Polar satellite and ground-based cameras, *Adv. Space Res.*, *23*, 1647–1652.
Fujii, R., N. Sato, T. Ono, H. Fukunishi, T. Hirasawa, S. Kokubun, T. Araki, and T. Saemundsson (1987), Conjugacies of pulsating auroras by all-sky TV observations, *Geophys. Res. Lett.*, *14*, 115–118.
Kelley, M. C. (1989), *The Earth's Ionosphere Plasma Physics and Electrodynamics*, Academic, San Diego, Calif.
Liou, K., P. T. Newell, D. G. Sibeck, C. I. Meng, M. Brittnacher, and G. Parks (2001), Observation of IMF and seasonal effects in the location of auroral substorm onset, *J. Geophys. Res.*, *106*, 5799.
Pulkkinen, T. I., D. N. Baker, P. K. Toivanen, J. S. Murphree, and L. A. Frank (1995), Mapping of the auroral oval and individual arcs during substorms, *J. Geophys. Res.*, *100*, 21,987–21,994.

Figure 5. (a) Snapshot of open (solid, dashed, dotted) field lines and one reconnected closed (thick) field line under the influence of the magnetic tension force (thick grey arrows) from IMF $B_y > 0$ and $B_z < 0$ acting toward dawn in the Northern Hemisphere and toward dusk in the Southern Hemisphere. (b) Superposition of the IMF and the symmetric field.
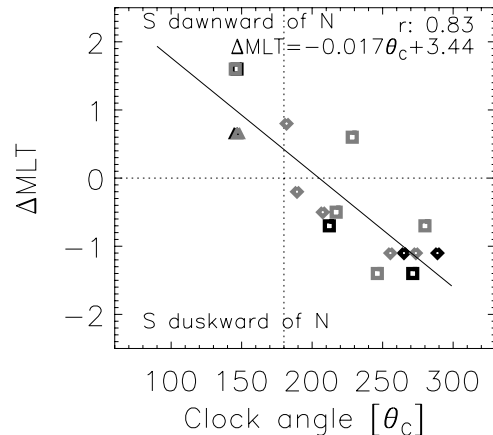
Richmond, A. D. (1995), Ionospheric electrodynamics using magnetic apex coordinates, *J. Geomagn. Geoelectr.*, *47*, 191–212.

Sandholt, P. E., and C. J. Farrugia (1999), On the dynamic cusp aurora and IMF B_y, *J. Geophys. Res.*, *104*, 12,461–12,472.

Sandholt, P. E., C. J. Farrugia, J. Moen, O. Noraberg, B. Lybekk, T. Sten, and T. Hansen (1998), A classification of dayside auroral forms and activities as a function of interplanetary magnetic field orientation, *J. Geophys. Res.*, *103*, 23,325–23,345.

Sato, N., R. Fujii, T. Ono, H. Fukunishi, T. Hirasawa, T. Araki, S. Kokubun, K. Makita, and T. Saemundsson (1986), Conjugacy of proton and electron auroras observed near l = 6.1, *Geophys. Res. Lett.*, *13*, 1368–1371.

Sato, N., T. Nagaoka, K. Hashimoto, and T. Saemundsson (1998), Conjugacy of isolated auroral arcs and nonconjugate auroral breakups, *J. Geophys. Res.*, *103*, 11,641–11,652.

Sibeck, D. G. (1985), The distant magnetotail's response to a strong interplanetary magnetic field B_y: Twisting, flattening, and field line bending, *J. Geophys. Res*, *90*, 4011.

Stenbaek-Nielsen, H. C., and A. Otto (1997), Conjugate auroras and the interplanetary magnetic field, *J. Geophys. Res*, *102*, 2223–2232.

Stenbaek-Nielsen, H. C., T. N. Davis, and N. W. Glass (1972), Relative motion of auroral conjugate points during substorms, *J. Geophys. Res.*, *77*, 1844–1852.

Stenbaek-Nielsen, H. C., E. M. Wescott, T. N. Davis, and R. W. Peterson (1973), Auroral intensity differences at conjugate points, *J. Geophys. Res.*, *78*, 659–671.

Toffoletto, F. R., and T. W. Hill (1989), Mapping of the solar wind electric field to the Earth's polar cap, *J. Geophys. Res.*, *94*, 329–347.

Toffoletto, F. R., and T. W. Hill (1993), A nonsingular model of the open magnetosphere, *J. Geophys. Res.*, *98*, 1339–1344.

Tsyganenko, N. A. (1998), Modeling of twisted/warped magnetospheric configurations using the general deformation method, *J. Geophys. Res.*, *103*, 23,551–23,563.

Tsyganenko, N. A. (2002a), A model of the near magnetosphere with a dawn-dusk asymmetry: 1. Mathematical structure, *J. Geophys. Res.*, *107*(A8), 1179, doi:10.1029/2001JA000219.

Tsyganenko, N. A. (2002b), Model of the near magnetosphere with a dawn-dusk asymmetry: 2. Parametrization and fitting to observations, *J. Geophys. Res.*, *107*(A8), 1176, doi:10.1029/2001JA000220.

Vorobjev, V. G., O. I. Yagodkina, D. Sibeck, K. Liou, and C. I. Meng (2001), Aurora conjugacy during substorms: Coordinated Antarctic ground and Polar Ultraviolet observations, *J. Geophys. Res.*, *106*, 24,579–24,591.

Wing, S., P. T. Newell, D. G. Sibeck, and K. B. Baker (1995), A large statistical study of the entry of interplanetary magnetic field component into the magnetosphere, *Geophys. Res. Lett.*, *22*, 2083–2086.

————————————

L. A. Frank and J. B. Sigwarth, Department of Physics and Astronomy, University of Iowa, Iowa City, IA 52242-1479, USA. (louis-frank@uiowa.edu; john-sigwarth@uiowa.edu)

H. U. Frey, T. J. Immel, S. B. Mende, and N. Østgaard, Space Sciences Laboratory, University of California, Berkeley, CA 94720-7450, USA. (hfrey@ssl.berkeley.edu; immel@ssl.berkeley.edu; mende@ssl.berkeley.edu; nikost@ssl.berkeley.edu)

T. J. Stubbs, Laboratory for Extraterrestrial Physics, NASA Goddard Space Flight Center, MC 690.4, Greenbelt, MD 20771, USA. (tstubbs@lepvax.gsfc.nasa.gov)
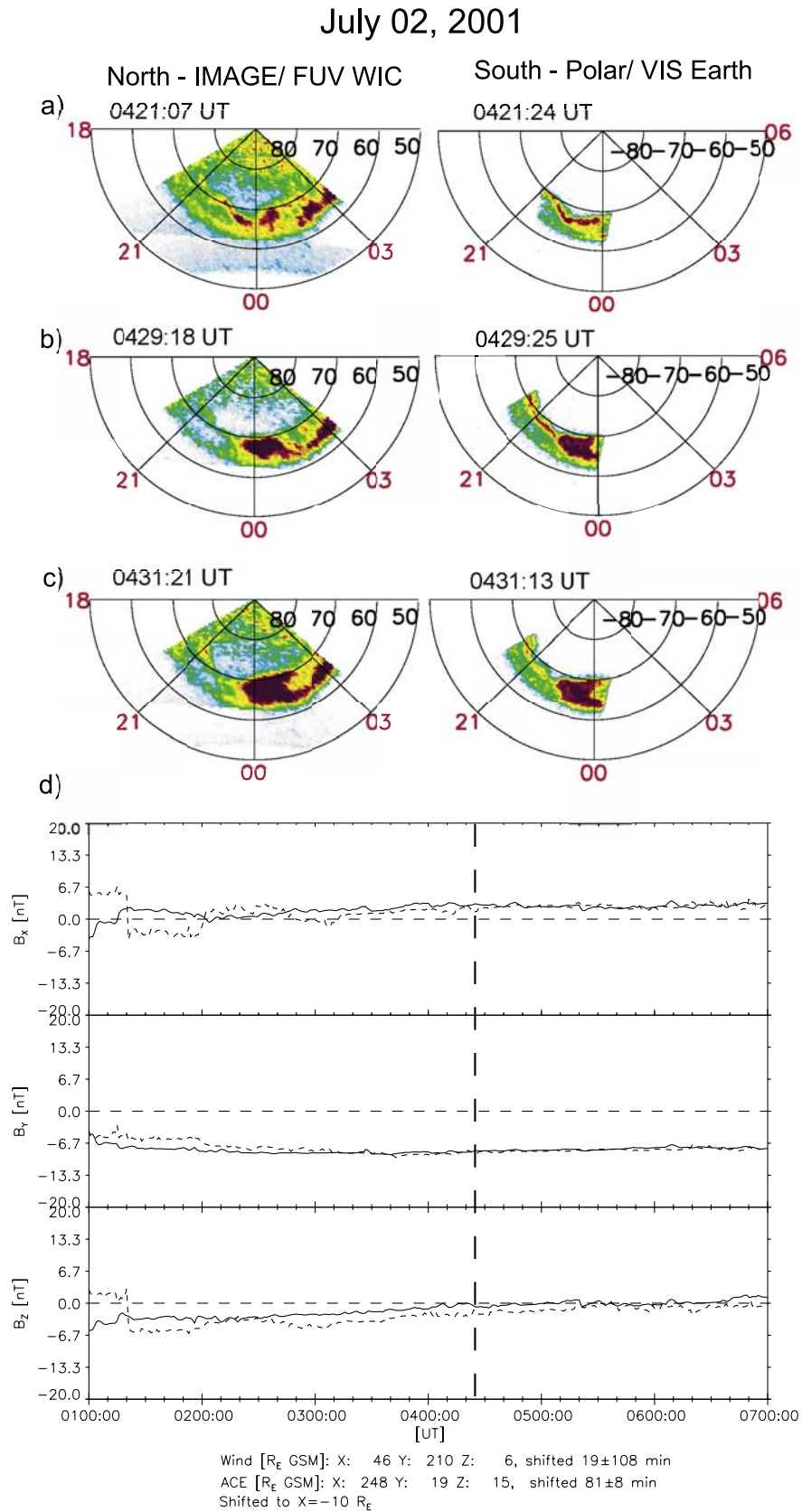
Figure 3. The 2 July 2001 event. (a)−(c) Images from the conjugate hemispheres. (d) IMF.